In Situ Polymer/Polymer Composites from Poly(ethylene terephthalate), Polyamide-6, and Polyamide-66 Blends

M. EVSTATIEV,[1] J. M. SCHULTZ,[2] S. PETROVICH,[1] G. GEORGIEV,[1] S. FAKIROV,[1] K. FRIEDRICH[3]

[1] Laboratory on Polymers, Sofia University, 1126 Sofia, Bulgaria

[2] Materials Science Program, University of Delaware, Newark, DE 19716

[3] Institute of Composite Materials, University of Kaiserslautern, 67663 Kaiserslautern, Germany

Received 2 January 1997; accepted 27 June 1997

ABSTRACT: *In situ* reinforced binary and ternary polymer/polymer composites are obtained by the melt blending of poly(ethylene terephthalate) (PET), polyamide-6 (PA-6), and polyamide-66 (PA-66) in an extruder in the presence of a catalyst, followed by drawing of the extrudate and annealing of the drawn blends. The blends were studied by DSC, X-ray, SEM, and mechanical testing. After drawing, all the components were found to be oriented, forming microfibrils with diameters of about 1–2 μm. The chemical nature of the homopolymers affects the blends' morphologies; while the PA-66/PA-6 blend is homogeneous, phase separation is established in the case of PET/PA-6. The decrease in the enthalpy of melting of the blend components as well as the depression of their peaks of crystallization from the melt, compared to pure homopolymers, are indications that block copolymers have been formed via interchange reactions during the blending process. On the one hand, these copolymers improve the compatibility of the homopolymers, and on the other hand, they alter the chemical composition of the blends. After thermal treatment at 245°C, i.e., above the T_m of PA-6, the latter undergoes some disorientation, while PET and PA-66 retain their microfibrillar shape, and in this way, a compositelike structure is created. The presence of chemical bonds between the separate phases via copolymers favors the cocrystallization of PA-66 and PA-6 as well as the cooperative crystallization of PET, PA-6, and PA-66, both modes fostering improved compatibility (adhesion) of the blend components. J Appl Polym Sci **67:** 723–737, 1998

Key words: polymer blends and composites; fibrillar reinforcement; compatibilization

INTRODUCTION

Altering the properties of commercial polymers via physical or chemical modification has been of increasing importance because of the lower costs involved relative to synthesizing new polymers. Blending of two or more homopolymers is an example of physical modification.

In the last few years, self-reinforced thermoplastic composites based on thermotropic liquid crystalline polymers (LCPs) and commercial engineering matrix resins have been studied.[1–6] They are produced by melt blending of the LCPs and the thermoplastic matrix, usually in an extruder, followed by a processing step (high elongational flow) in which LCPs are known to form

Correspondence to: J. M. Schultz.

Contract grant sponsor: National Science Foundation; contract grant number: INT-9307812; contract grant sponsor: Bulgarian Ministry of Education and Science; contract grant number: X-542; contract grant sponsor: Deutsche Forschungsgesellschaft; contract grant number: FR 675/21-1.

Journal of Applied Polymer Science, Vol. 67, 723–737 (1998)
 CCC 0021-8995/98/040723-15

in situ microfibrils that serve as the reinforcing element (phase). The aspect ratio and adhesion (compatibility) between the microfibrillated LCP and the matrix are of prime importance for the mechanical properties of these *in situ* composites. In turn, the aspect ratio depends on the processing conditions (extensional flow) and compatibility, the latter being directly related to the chemical nature of the homopolymers in the blend.

A new type of polymer/polymer composite (the so-called microfibrillar composites [MFCs]), which satisfies to a great extent the above-mentioned peculiarities (aspect ratio and compatibility) of the LCP-reinforced composites, has recently been developed.[7–11] MFCs are formed by the melt blending of two or more immiscible thermoplastic polymers, cold or hot drawing, and annealing of the drawn blend. Upon drawing, the components of the blend are oriented and microfibrils of the minor, higher melting component are formed. The structure of the material is further developed by subsequent heat treatment, and the temperature and duration of this processing step have been shown to significantly affect the structure and properties of the blend. If the heat-treatment temperature (T_a) is set below the melting point (T_m) of both components, the microfibrillar structure imparted by drawing is preserved and further improved as a result of physical processes, such as additional crystallization, minimization of defects in the crystalline regions, and relaxation of residual stresses in the amorphous regions. On the other hand, if T_a is set between the melting temperatures of the two components, melting of the lower-melting polymer takes place, forming an isotropic, relaxed matrix, while the microfibrillar regions, involving the component with higher T_m, preserve their orientational and morphological characteristics. The resulting material is referred to as a microfibrillar-reinforced composite.

With respect to the size of the reinforcing elements, MFCs take an intermediate position between the two extreme groups of polymer composites: macrocomposites (e.g., fiber-reinforced composites) and molecular composites with LCPs as reinforcing elements. Bundles of highly oriented microfibrils play the role of reinforcing elements in MFCs. The latter exhibit mechanical properties comparable to those of short glass fiber-reinforced engineering thermoplastics.[7–11]

In addition to physical changes, the thermal treatment of blends of semicrystalline and/or amorphous condensation polymers might involve chemical changes, which, in turn, affect the compatibility of the components. In fact, exchange reactions between adjacent functional groups, generating *in situ* copolymers, are reported to be a possible method for compatibilizing polyesters and polyamides.[12–15] Solid-state reactions in linear polycondensates are particularly favored at high annealing temperatures and occur in the noncrystalline phases, which enjoy relatively higher mobility.[16] Evidence for solid-state exchange reactions and additional condensation were observed with binary and ternary blends of poly(ethylene terephthalate) (PET), poly(butylene terephthalate) (PBT), and polyamide-6 (PA-6), after the samples were heat-treated at 240°C.[7–11] Mainly, a decrease in the degree of crystallinity and the enthalpy of melting of the thermally treated samples were observed by DSC and WAXS; these changes were essentially caused by the diminishing contribution of the PA-6 and/or the PBT component. This weaker ability of the PA-6 and PBT components to crystallize in thermally treated PET/PA-6 and PET/PBT/PA-6 blends was attributed to their chemical interaction in the molten state, during annealing, with the amorphous fractions of PET to form PET-PA-6 and PET-PA-6-PBT copolymers at the interfaces between the amorphous matrix and microfibrillar regions. Prolonged annealing has two effects: (i) growth of the copolymer layers to eventually involve the entire lower-melting PA-6 matrix, and (ii) transformation of the originally formed block copolymers into entropically favored random copolymers which by themselves are noncrystallizable upon cooling. The formation of copolymer layers, improving the adhesion and compatibility between microfibrils and matrix, was also supported by the response of the resulting MFC to external mechanical fields.[7–11]

The purpose of this work was to extend the technique of MFC preparation to different polymer blends, as well as to study the improvement of compatibility during melt blending with the addition of a catalyst. As already mentioned, the *in situ* generation of copolymers during extrusion is a useful means for compatibilizing polyesters and polyamides.[13–15] Blends of PET/PA-6, polyamide-66 (PA-66)/PA-6, and PET/PA-6/PA-66 in weight ratios of 40/60, 40/60, and 20/60/20, respectively, are used. These specific polymers are chosen because of their great commercial importance for the large-scale production of composites, fibers, and films. An attempt is made to study the super-

molecular organization and its contribution to the properties of binary and ternary blends of PET, PA-6, and PA-66 with different thermal prehistory.

EXPERIMENTAL

Materials and Processing

Commercial engineering-grade polymers PET (Vidlon, Bulgaria), PA-6 (Vidamid, Bulgaria), and PA-66 (Ultramid, BASF, Germany) were dried in an oven at 120°C for 24 h. Pellets of these homopolymers were mixed in weight ratios of PET/PA-6 = 40/60, PA-66/PA-6 = 40/60, and PET/PA-6/PA-66 = 20/60/20, by the addition of *p*-toluenesulfonic acid as a catalyst in an amount of 0.35% based on the weight of PA-6. These weight ratios correspond approximately to the following volume ratios: 35/65, 40/60, and 17/62/21, respectively.

Blending was performed on a Brabander single-screw (30 mm diameter) lab extruder at 15–20 rpm. The extrudate from a 2 mm capillary die was immediately quenched in a water bath at 15°C. The temperature zones in the extruder were 285, 290, 295, 300, and, finally, 310°C at the die.

Extruded bristles from all blends were drawn at room temperature on a Zwick 1464 machine at a strain rate of 50 mm min^{-1} to a draw ratio $\lambda = 3.4–3.6$ and diameter of about 1 mm and then flushed with hot air (60–65°C) to remove internal strains. Some of the drawn samples were then subjected to isothermal annealing with fixed ends at 245°C for 100 min in a vacuum (0 in. Hg). The sample preparation conditions are given in Table I.

Differential Scanning Calorimetry

Measurements of all samples (of almost equal weight of 17–18 mg) were carried out on a Perkin-Elmer DSC 7 thermoanalyzer at a heating and cooling rate of 10°C min^{-1}. After keeping the sample at a maximum temperature of 290°C for 10 s, nonisothermal crystallization from the melt was performed. The samples thus crystallized were subjected to a second heating. The respective thermograms served for the determination of the heats of fusion of the homopolymers in the blends during the first ($\Delta H_f'$) and the second ($\Delta H_f''$) melting. Nonisothermal crystallization from the melt produced values of the heat of crystallization (ΔH_c) of the homopolymers in the blends. The degree of crystallinity w_c(DSC) of homopolymers and their fractions in the blends was determined according to the equation $w_c(\mathrm{DSC}) = \Delta H_f / F\Delta H^0$, where ΔH_f is the heat of fusion, and F, the homopolymer weight fraction in the blend, using for the ideal heats of fusion of the respective homopolymers the following values: ΔH^0(PET) = 140 kJ/kg,[17] ΔH^0(PA-6) = 230 kJ/kg,[18], and ΔH^0(PA-66) = 300 kJ/kg.[18]

X-ray Diffraction

X-ray diffraction was carried out in a Warhus flat-film camera, using Ni-filtered CuKα radiation and a 4 cm specimen-to-film distance.

Scanning Electron Microscopy

A JEOL JSM 5400 scanning electron microscope, operating at an accelerating voltage of 25 kV, was used for the observation of differently prepared specimens. Cryogenic (i.e., brittle) fracture surfaces were obtained by breaking the specimens while immersed in liquid nitrogen. Other specimens were obtained by peeling back the outer, highly oriented skin of the drawn and annealed bristles, thereby exposing the structure of the core. Specimens for microfibrillar observation were prepared by extraction of PA-6 and PA-66 from the drawn blends, using formic acid for 25 h. All specimens were then mounted and coated with gold before analysis.

Mechanical Testing

Mechanical tests were carried out at room temperature and a strain rate of 5 mm min^{-1} using an Instron 4201 tensile tester. The Young's modulus (E), tensile strength (σ_t), and ultimate strain (ε_u) were determined from the load-extension curves. All values are averaged from five measurements.

RESULTS

Thermal Behavior

DSC thermograms of pure homopolymers and blends in the as-extruded, as-drawn, and additionally annealed states are shown in Figures 1–4. The scans of Figure 1 are over a range (0–100°C) suitable to establish the glass transition temperature. The other scans are over a larger

Table I Sample Preparation Conditions

Sample	Draw Ratio (λ)	Annealing in Vacuum with Fixed Ends	
		T_a (°C)	t_a (min)
PET	—	—	—
PA-6	—	—	—
PA-66	—	—	—
PET/PA-6 blend (40/60 by wt)			
A	As extruded	—	—
A-0	3.5	—	—
A-1	3.5	245	100
PA-66/PA-6 blend (40/60 by wt)			
B	As extruded	—	—
B-0	3.6	—	—
B-1	3.6	245	100
PET/PA-6/PA-66 blend (20/60/20 by wt)			
C	As extruded	—	—
C-0	3.4	—	—
C-1	3.4	245	100

temperature range, in order to establish melting and crystallization behavior. As can be seen in Figure 1(a), as-extruded PET/PA-6 and PET/PA-6/PA-66 blends exhibit two glass transitions (T_g) at about 50°C for PA-6 and PA-66 and at 75°C for PET. The fact that the blends have two glass transitions indicates that their components are immiscible. On the contrary, the PA-6/PA-66 blend reveals just one, quite broad T_g, suggesting some miscibility of the two polyamides[19] [Fig. 1(a), sample B]. However, after drawing, the lower T_g tends to disappear while the T_g of PET shifts to lower temperatures [Fig. 1(b), samples A-0 and C-0]. This observation could be related to an improvement of the components' compatibility as a result of drawing.[13] The latter leads to alignment and strengthening of the chains as well as to stress-induced crystallization. The additional thermal treatment of the drawn blends [Fig. 1(b), samples A-1 and C-1] results in the appearance of a single glass transition, shifted to lower temperatures.

Figure 2 shows thermograms obtained during the first heating to 290°C. It is seen that the as-extruded and as-drawn blends exhibit very broad but clearly expressed exothermic peaks in the range of 90–180°C. Small but well-shaped crystallization peaks are observed with samples A and C [Fig. 2(a)] at about 115°C. These exotherms are likely due to the cold crystallization of the PET component in the PET/PA-6 and PET/PA-6/PA-66 blends. The absence of crystallization peaks in the PA-6/PA-66 blend [Fig. 2(a), sample B] supports this assumption.

The general trend of the thermograms during heating of the as-extruded and as-drawn blends suggests a metastable state of these systems, undergoing considerable change during heating in the calorimeter. These changes are mostly related to relaxation and crystallization, leading, in turn, to separation of the blend components, as can be concluded from the separate melting peaks. In this respect, sample B (PA-66/PA-6 blend) is an exception, since the melting peak for the PA-6 component is poorly expressed [Fig. 2(a)].

The trend of the curves obtained with the blends annealed at 245°C (above the melting of PA-6) suggests a perfecting of the structure of the higher-melting PET and PA-66 components, compared to the as-extruded and as-drawn samples (Fig. 2). It is seen in Table II, where the data from DSC measurements are presented, that the heats of fusion during the first melting (ΔH_f) as well as the degrees of crystallinity w_c(DSC) of the PET, PA-66, and PET + PA-66 fractions in the annealed blends (samples A-1, B-1, and C-1) are

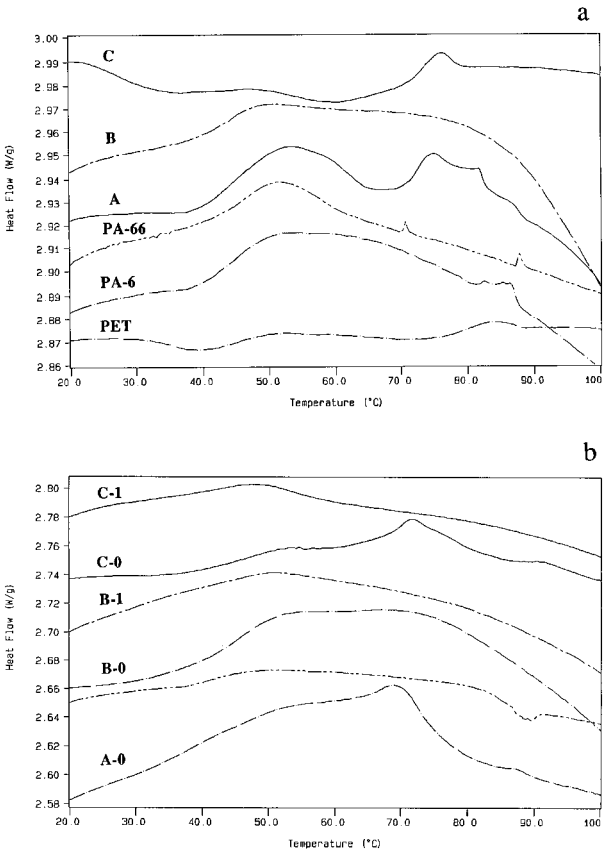

Figure 1 DSC thermograms of neat PET, PA-6, PA-66, and their blends taken at the very beginning of the first heating (up to 100°C): (a) as-extruded; (b) as-drawn and drawn and annealed blends. For sample designation, see Table I.

much higher than the respective values for the as-extruded and as-drawn materials. On the other hand, T_m, ΔH_f, and w_c(DSC) of the PA-6 fractions in the same blends are lower than the respective values for the as-drawn blends (Table II). We have already observed a similar behavior of the PA-6 component in PET/PA-6 (1 : 1 by wt) and PET/PA-6/PBT (1 : 1 : 1 by wt) blends with no catalyst added, but after much longer annealing at 240°C.[7–9]

Due to the higher crystallizability of PA-6 and PA-66 as well as to the prolonged drying, low-temperature crystallization ("cold crystallization") peaks are not observed with the starting homopolymers [Fig. 2(a)]. This could be also the reason for the appearance of two PET melting peaks (at 238 and 258°C). After melt blending, the lower-temperature PET melting peak is not observed (Fig. 2).

The outstanding feature of the second cooling DSC scans is the presence of only one crystallization endotherm. In Figure 3(a) are shown scans from the neat polymers and from the as-extruded blends. The as-extruded A and C blends each show only one exotherm. Those exotherms lie at temperatures between those of the neat polymer components. Blend B, the PA-6/PA-66 blend, exhibits one major endotherm centered near 215°C and also a broad, weaker endotherm centered near 195°C. The cooling curves for the specimens after drawing and after heat treatment likewise exhibit only one endotherm each.

In contrast, upon reheating, the blends each exhibit two melting endotherms, and these lie near but somewhat lower than the positions of the endotherms for the neat polymers. This behavior is shown in Figure 4.

A broadening of the crystallization temperature ranges (T_c) and a decrease in the intensity of the exotherms are observed with all blends, compared to those of the respective homopoly-

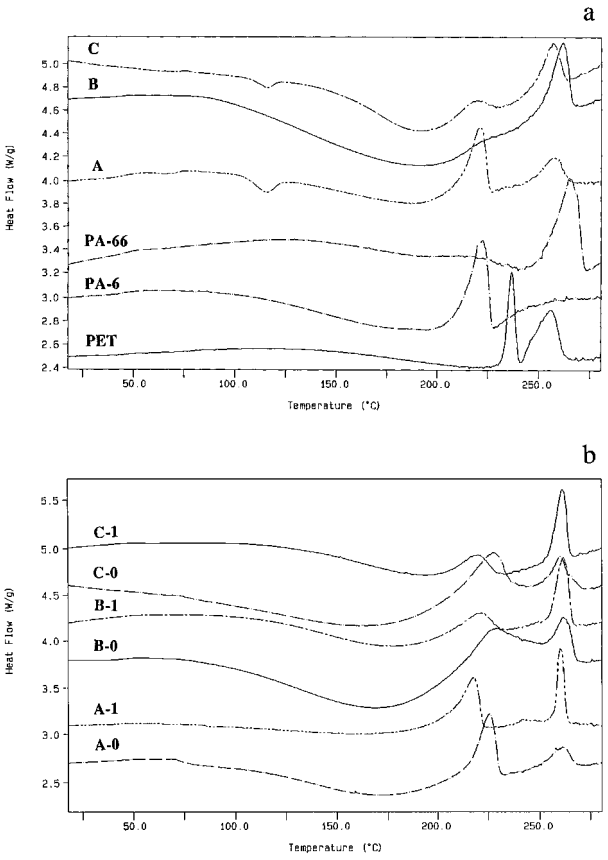

Figure 2 DSC thermograms of neat PET, PA-6, PA-66, and their blends taken at the first heating: (a) as-extruded; (b) as-drawn and drawn and annealed blends. For sample designation, see Table I.

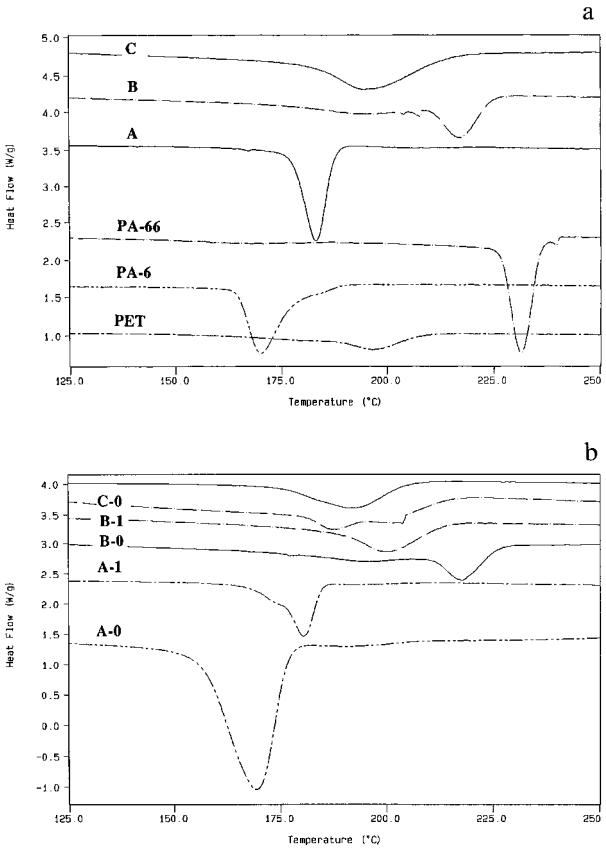

Figure 3 DSC crystallization curves of the same samples as in Figure 2 taken during cooling: (a) as-extruded; (b) as-drawn and drawn and annealed blends.

mers. The behavior of the PET/PA-66 blend is somewhat exceptional [Figs. 3(a) and (b), samples A and A-0]; however, after annealing at 245°C, the exotherm intensity (ΔH_c) of this blend also decreases. These results and analogous results relating to second melting are shown in Table II.

Orientation

Qualitative trends in orientation can be seen in the X-ray diffraction results. In Figure 5 are shown the flat-film patterns obtained from compositions A, B, and C, each for the as-extruded state, after drawing, and after drawing plus heat treatment at 245°C. All phases of all compositions are isotropic (i.e., exhibit complete Debye rings) in the as-extruded state. After drawing, all phases are highly oriented, with chains strongly aligned along the bristle axis.

However, after heat treatment, there are important differences among the blends. The PET/PA-6 blend shows PET to be still highly oriented, as evidenced from the PET $hk0$ spots being lying on the equator. In contrast, the PA-6 reflections appear as extended arcs (still centered on the equator). The PA-6 matrix is clearly much less oriented than the PET fibrils. For the PA-6/PA-66 blend, the diffraction arcs for the two materials overlap and cannot be distinguished. All $hk0$ diffraction is highly concentrated at the equator, indicating relatively little randomization of the matrix. The degree of misorientation is, however, manifestly greater than for the as-drawn state. The ternary blend likewise shows some orientational disorder of the matrix PA-6, but not a complete isotropization.

Morphology

Scanning electron micrographs of the cryogenic fracture surfaces of the as-extruded, as-drawn, and isotropized PET/PA-6, PA-6/PA-66, and PET/PA-6/PA-66 blends are shown in Figure 6.

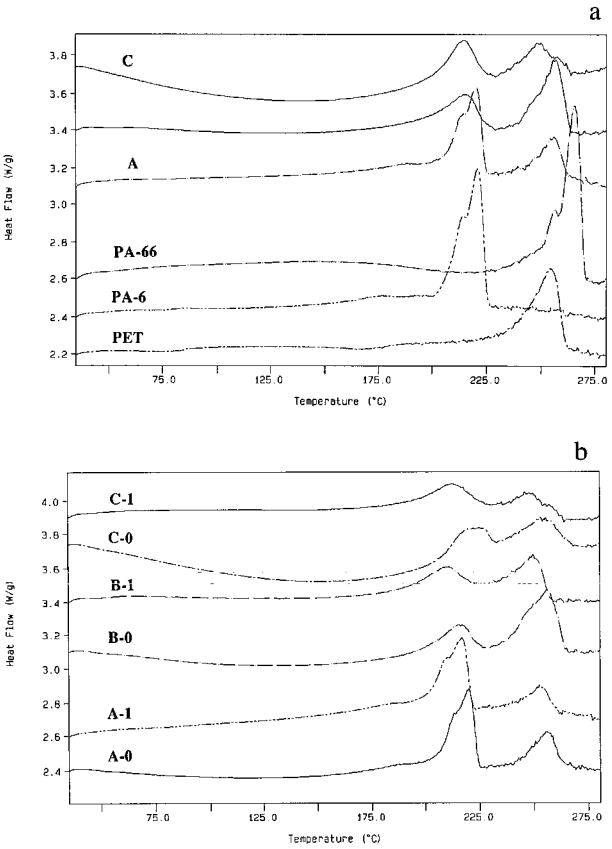

Figure 4 DSC thermograms of the same samples at the second heating: (a) as-extruded; (b) as-drawn and annealed blends.

Table II DSC Data of Pure Homopolymers and of the PET/PA-6, PA-66/PA-6, and PET/PA-6/PA-66 in First Heating, Cooling, and Second-heating Modes

		First Heating			Crystallization	Second Heating		
	T_g (°C)	T_m (°C)	ΔH_f (kJ/kg)	w_c (DSC)	T_c (°C)	T_m (°C)	ΔH_f (kJ/kg)	w_c (DSC)
PET	81	238 + 258	53	0.38	199	256	39	0.27
PA-6	52	223	52	0.22	171	216 + 222	52	0.22
PA-66	51	266	54	0.19	231	258 + 266	59	0.20
PET/PA06		PA-6 PET	PA-6 PET	PA-6 PET		PA-6 PET	PA-6 PET	PA-6 PET
A	52 + 75	221 257	61 22[a]	0.26 0.16	183	215 + 221 257	48 35	0.21 0.25
A-0	68	225 261	60 32	0.26 0.23	170	218 + 220 256	47 32	0.20 0.21
A-1	51	217 260	43 50	0.18 0.36	181	209 + 216 252	45 17	0.20 0.11
PA-66/PA-6		PA-6 PA-66	PA-6 PA-66	PA-6 PA-66		PA-6 PA-66	PA-6 PA-66	PA-6 PA-66
B	50	— 261	— 55	— 0.18	217 + 195	216 257	23 66	0.10 0.22
B-0	53	226 262	35 53	0.15 0.18	216 + 195	217 257	22 71	0.10 0.23
B-1	50	219 261	20 75	0.08 0.25	198	211 250	16 40	0.06 0.13
PET/PA-6/PA-66		PA-6 PET + PA-66	PA-6 PET + PA-66	PA-6		PA-6 PET + PA-66	PA-6 PET + PA-66	PA-6
C	49 + 75	217 256	20 45[a]	0.08	195	215 248 + 256	23 45	0.10
C-0	52 + 72	227 260	36 45	0.17	206 + 188	218 253 + 256	22 32	0.10
C-1	48	220 261	20 70	0.08	192	212 250 + 256	16 18	0.06

[a] $\Delta H_f - \Delta H_c$.

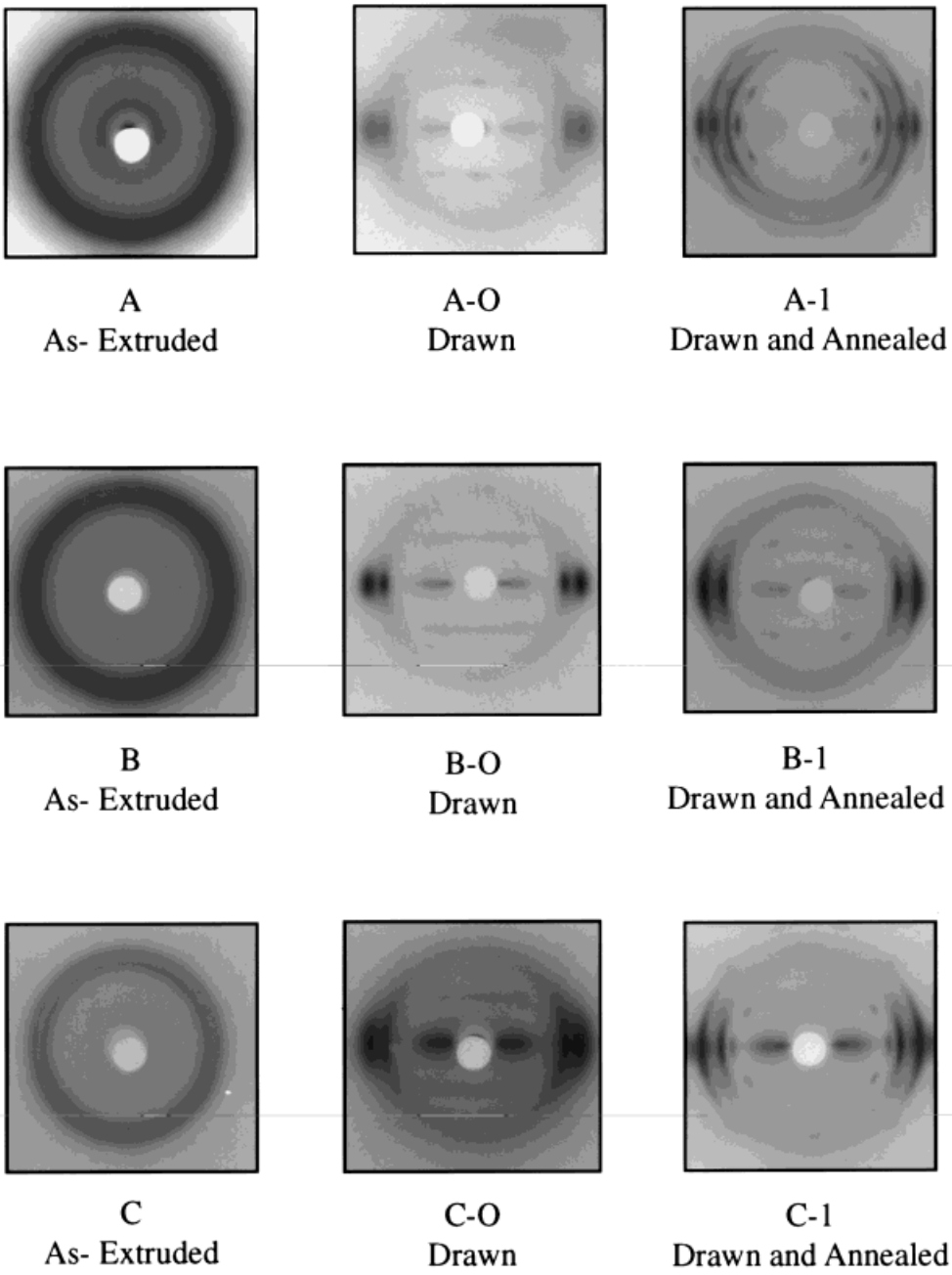

Figure 5 WAXS transmission patterns of PAT/PA-6, PA-66/PA-6, and PET/PA-6/PA-66 blends.

These specimens were prepared by fracturing perpendicularly to the bristle axis in liquid nitrogen. It should be noted that the samples behaved differently during the fracturing, suggesting different morphologies of the blends studied. The as-extruded blends broke exactly perpendicularly to the bristle axis, while the as-drawn and isotropized samples split along the draw direction. The SE micrographs of these samples are taken from precisely these surfaces.

It is seen in Figure 6 that the PET component in the as-extruded PET/PA-6 blend is relatively uniformly dispersed in the PA-6 medium in the form of a large number of eliptic particles (diameters of 3–5 μm). Holes of the same shape and size are also observed; so it can be concluded that they

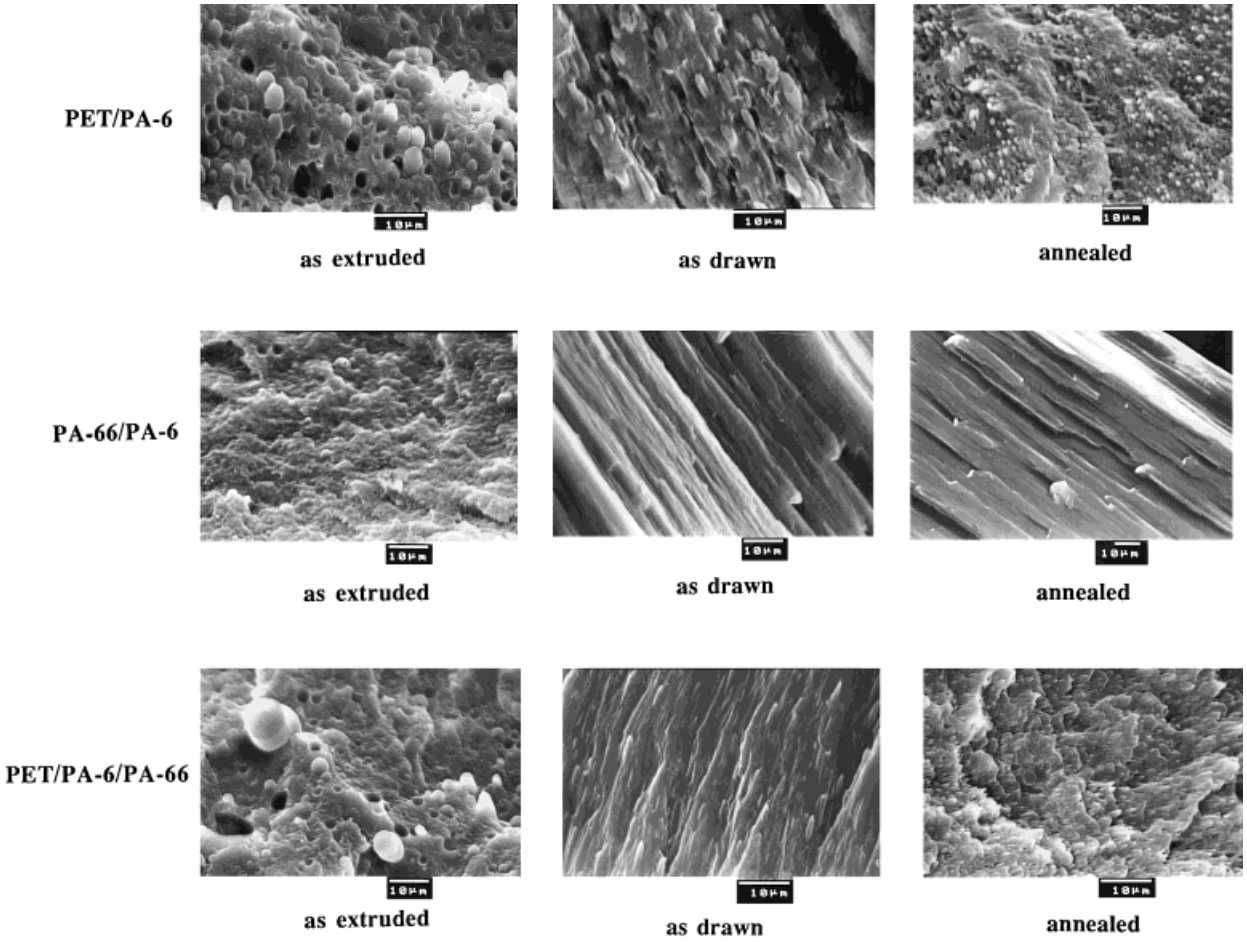

Figure 6 SEM micrographs of PET/PA-6, PA-66/PA-6, and PET/PA-6/PA-66 blends. Specimens broken at a cryogenic temperature.

result from the pullout of PET particles during cryogenic fracture.

The morphology of the as-extruded PA-6/PA-66 blend is somewhat different. It is seen in Figure 6 that this sample has a homogeneous structure, with just a small number of spherical particles and holes. This homogeneity is most probably due to the compatibility of the two polyamides.

The fracture surface pattern of the as-extruded PET/PA-6/PA-66 blend takes an intermediate position between the two cases discussed above; it represents a homogeneous PA-6 + PA-66 continuous medium with PET as the dispersed phase. Here, however, the PET particles reveal a more elongated shape and their volume fraction is smaller.

Subsequent drawing results in drastic changes of the blends' morphologies (Fig. 6). As seen from the fracture surface of the as-drawn PET/PA-6 blend, microfibrils are generated *in situ*. It should be noted that PET and PA-6 fibrils differ in morphology: The former (the lighter particles, with diameters of 1–2 μm) are inserted in a continuous, oriented PA-6 phase. After isotropization of the PA-6 component at 245°C, the structure of PET remains almost unchanged—the axially oriented PET fibrils are now inserted in an isotropic PA-6 matrix, i.e., a typical composite structure is observed.

The morphology of the as-drawn PA-6/PA-66 blend is substantially different; a layer-like structure is seen in Figure 6. This structure is preserved after heat treatment as well, and the reason for this morphological peculiarity should be again the miscibility of the two polyamides.

The morphology of the as-drawn PET/PA-6/PA-66 blend again takes an intermediate position between the two other blends. Figure 6 clearly

reveals separate PET fibrils inserted in a continuous, fibrillized PA-6 + PA-66 medium. After annealing at 245°C, the morphology of this sample becomes close to that of the PET/PA-6 blend (Fig. 6). However, the latter reveals a relatively larger number of holes resulting from fibril pull-out. On the one hand, this can be attributed to the higher volume fraction of PET in the PET/PA-6 blend, but, more importantly, it is an indication of a better interfacial adhesion between the fibrils and the PA-6 matrix in the case of the PET/PA-6/PA-66 blend. It should be noted that the best interfacial adhesion between the components is observed with the PA-6/PA-66 blend after annealing at 245°C. For this reason, the fibrillized PA-66 phase is completely included in the partially disoriented PA-6 medium and cannot be observed separately (Fig. 6).

Micrographs of peeled surfaces of as-drawn and annealed PET/PA-6, PA-66/PA-6, and PET/PA-6/PA-66 blends are shown in Figure 7. It is seen that the morphologies of the as-drawn PET/PA-6 and PET/PA-6/PA-66 samples are almost identical, representing continuous PA-6 or PA-6 + PA-66 phases in which PET fibrils, oriented in the draw direction, are distributed. The micrographs in Figure 7, of PET/PA-6 samples in which the polyamide fractions are extracted, reveal that the PET fractions in these blends represent separate fibrils with diameters of about 1 μm or bundles of fibrils.

The as-drawn PA-66/PA-6 blend has a layerlike structure, and separate microfibrils are not observed (Fig. 7). This result aligns with the observation that both components remain highly oriented after heat treatment. This X-ray diffraction result hints that there should not be easily differentiable fibril and matrix phase regions. Microfibrils are, however, found on the bristles' surfaces (Fig. 7), where the state of stress is likely higher than in the interior. It should be noted that the PET/PA-6 and PET/PA-6/PA-66 bristles' surfaces have a similar morphology.

Mechanical Properties

Static mechanical properties of all blends are shown in Table III. It is seen that the as-drawn samples have Young's modulus (E) values that are four to five times higher than those of the as-extruded samples. This holds also for the values of the tensile strength (σ_t) where the difference is even greater, i.e., seven to nine times. It should be noted, however, that while the σ_t of the as-drawn PET/PA-6 blend (Table III, sample A-1) is almost identical to the tensile strength of the same blend with a 1 : 1 weight ratio of the components, the E value is lower by about 35%.[8] This is probably due to the different weight ratios of the components as well as to the fact that in the present case E is calculated from the straight portion of the load-extension curve (deformation from 0 to 5%), while in Ref. 8, E is defined in the deformation range from 0.05 to 0.5% using an incremental extensiometer. The same samples show from 3.6 to 6 times lower ultimate strain (ε_u) than do the as-extruded blends.

After heat treatment, i.e., after isotropization, E and σ_t decrease by 18–20% and 52–55%, respectively, compared to these mechanical parameters of the as-drawn blends, while the ultimate strain increases by 30–50%. Nevertheless, the modulus and strength of the heat-treated samples are three to four times higher than those of the as-extruded starting blends (Table III).

DISCUSSION

Compatibilization

As already mentioned, exchange reactions between adjacent groups are reported to be a possible method for improvement of compatibility of immiscible linear polycondensates.[12–15] Pillon and Utracki[15] reported 5–23% conversion in the PET/PA-66 blend during a single pass through an extruder, catalyzed with 0.2% p-toluenesulfonic acid. This percentage is quite high, taking into account that the conversion amounts to about 1% if one ester–amide reaction occurs per macromolecule.

The blends studied here are obtained by extrusion parameters that are very similar to those reported in Ref. 15 (temperature of 280–310°C, 0.35% by wt of the same catalyst and residence time of about 5 min), so one could assume the occurrence of some degree of conversion, i.e., the formation of binary and/or ternary copolymers. The chemical changes in polymer blends affect some physical properties of the homopolymers, and by following some purely physical parameters, one can indirectly establish the occurrence of these chemical changes. A typical example in this respect is the decreased crystallizability of the homopolymers in the blends, which, in the present cases, is revealed by (i) the broadening of the T_c peaks and the decrease in intensity of the

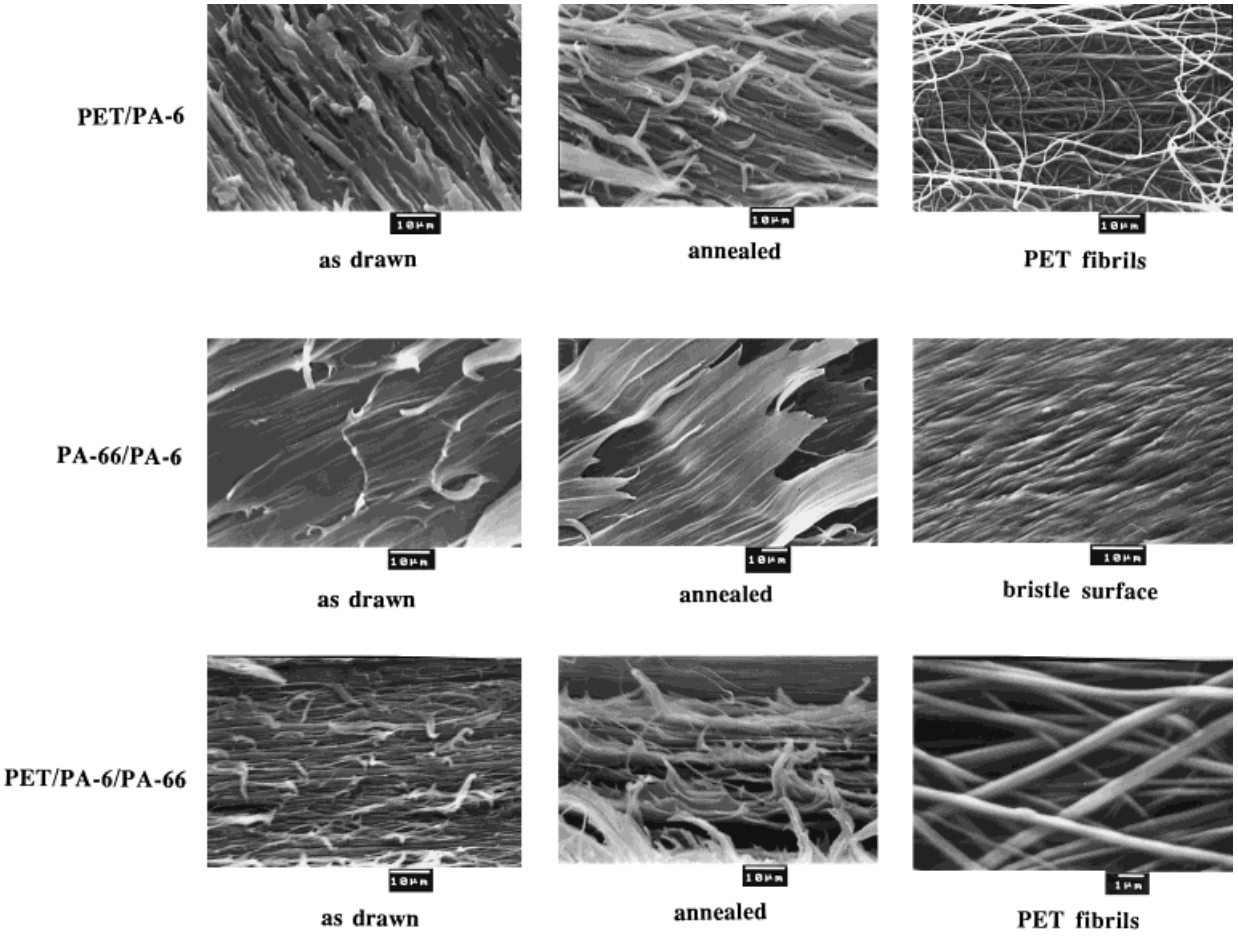

Figure 7 SEM micrographs of PET/PA-6, PA-66/PA-6, and PET/PA-6/PA-66 blends. Specimens obtained by removing PA-6 and PA-66 (peeling or selective extraction) from the drawn blends.

exotherms of the blends compared to those of the respective homopolymers and (ii) the doubly lower values of the normalized heats of fusion at the second heating $\Delta H_f''$ of the PA-6 component in the PA-66/PA-6 and PET/PA-6/PA-66 blends, compared to pure PA-6 (Figs. 3 and 4 and Table II). The decrease of $\Delta H_f''$ of PA-6 in the PET/PA-6 blends is substantially smaller; in this case, however, a slight diminishing of $\Delta H_f''$ of the PET component is established. A similar trend is observed even in the first melting of these samples (Table II). The different values of $\Delta H_f'$ and $\Delta H_f''$ of the PA-6 component could be attributed to the difference in its supermolecular organization which is anisotropic at the first melting and isotropic at the second. After thermal treatment at 245°C of the oriented samples, an additional decrease of $\Delta H_f''$ and w_c(DSC) is observed with all blend components (A-1, B-1, and C-1 in Table II and Fig. 4). It should be noted, however, that the $\Delta H_f''$ values of the PET, PA-66, and PET/PA-66 fractions are much lower than their respective $\Delta H_f'$ values in the annealed blends. Once again, these differences result from the supermolecular organization; the additional thermal treatment leads to considerable perfection of the PET and PA-66 crystallites, and hence, to an increase in their ΔH_f values. In addition to crystallite perfection, ester–amide and amide–amide interchange reactions between fibrillar PET and PA-66 (i.e., in the solid state) and the melted PA-6 and/or copolymer matrix also take place under these conditions. Due to the presence of a catalyst, these chemical interactions are much faster than in the cases of uncatalyzed binary and ternary PET, PBT, and PA-6 blends treated in the same way.[7–11]

The formation of new block copolymers during additional thermal treatment, as well as the

Table III Mechanical Properties of As-extruded, As-drawn, as well as Drawn and Annealed PET/PA-6, PA-66/PA-6, and PET/PA-6/PA-66 Blends Determined in a Static Mode

Sample	Young's Modulus (E, GPa)	Tensile Strength (σ_t, MPa)	Ultimate Strain (ε_u, %)
PET/PA-6			
A (as-extruded)	1.41	39[a]	252
A-1 (as-drawn)	6.66	311	44
A-2 (annealed)	5.14	137	98
PA-66/PA-6			
B (as-extruded)	0.98	36[a]	266
B-1 (as-drawn)	3.83	315	61
B-2 (annealed)	3.14	134	106
PET/PA-6/PA-66			
C (as-extruded)	1.24	42[a]	237
C-1 (as-drawn)	5.18	298	64
C-2 (annealed)	4.12	132	92

[a] Yield strength.

changes in the length of those formed during extrusion, alter the chemical structure and the physical properties of the homopolymers. The considerably higher T_m and ΔH_f values of PA-6 in the PET/PA-6 blend, compared to its respective fractions in the PA-66/PA-6 and PET/PA-6/PA-66 samples, suggest the presence of much longer PA-6 blocks as well as of some amount of unreacted homopolymer. This assumption is supported also by the stronger disorientation and partial isotropization of the PA-6 phase in sample A-1 after the additional thermal treatment, as can be seen in Figure 5.

The chemical nature of the homopolymer partners plays an important role in the formation of the structure of the blends, thus influencing their properties as well. Due to their almost identical chemical structure, PA-6 and PA-66 are practically miscible,[19] as indicated by the presence of just one T_g and the homogeneity (no visible phase boundary) of the PA-66/PA-6 blend (Table II, Figs. 1, 6, and 7). These same figures reveal the presence of a phase boundary between PET and PA-6 and/or PA-66 in the PET/PA-6 and PET/PA-6/PA-66 blends; two glass transitions are observed which merge into one only after additional mechanical and thermal treatment, i.e., after additional ester–amide exchange reactions (Table II and Fig. 1).

Another important property of the blends studied is the so-called cooperative crystallization. Utracki et al.[20] reported association and cocrystallization between the two components in a PET/PA-66 blend. This is apparently not correct. The presence of one crystallization exotherm and two or more melting endotherms (Figs. 3 and 4 and Table II) is the fingerprint of cooperative crystallization.[21,22] In such cooperative crystallization in blends, crystals or crystal colonies grow separately (no cocrystallization) but with a common growth front. One envisions adjacent crystals or colonies growing in parallel. In the present case, the cooperation is likely enforced by exchange reactions, inducing chemical bonding between the phases; because of this bond, the components are required to develop in concert. Cooperative crystallization is most strongly expressed in the heat-treated samples, since they should have the largest number of chemical bonds between the homopolymers (Table II).

It is to be noted additionally that the melting points of PA-66 in blends B and C are depressed (particularly at the second heating mode), relative to neat PA-66 (Table II). This effect is likely the result of a degree of cocrystallization (solid solubility) of PA-6 in PA-66. Cocrystallization is extremely rare in polymer blends. It was observed with miscible PBT/poly(ether ester) blends, in which the poly(ether ester) is based on PBT and poly(ethyelene glycol).[23,24] Partial cocrystallization, i.e., epitaxial growth of PBT crystallites from a poly(ether ester) on homo-PBT crystallites in the respective blend, has also been reported.[25] The relatively higher values of ΔH_f, and w_c(DSC) of the PA-66 fraction in samples B and B-0 compared to neat PA-66 are another indication of cocrystallization between the two polyamides in this blend. It is likely that some degrees of copolymerization

and cocrystallization have prevented the PA-6 fraction from responding independently to the thermal treatment of the blend. This is supported also by the preservation of some orientation in the PA-6 fraction of the samples annealed at 245°C (Fig. 5).

Fibrillar Reinforcement

The fibril can be defined as a structural entity with material properties that are biased predominantly along a linear dimension or symmetry axis.[26] A prerequisite for the creation of such a structure in polymers is the stretching and alignment of the chains in the axial direction. This is usually achieved by drawing and orientation.

In situ generation of polymer microfibrils after cold drawing of the isotropic blends is shown in Figures 6 and 7. The different morphology of the drawn samples results from the different miscibility of the homopolymers. The total immiscibility of PET and PA-6 or PA-66 provides the possibility of observation of separate PET fibrils with a very good aspect ratio. In the as-drawn PET/PA-6 and PET/PA-6/PA-66 blends, PET fibrils with a diameter of about 1–2 μm are inserted into a continuous, oriented PA-6 or PA-6 + PA-66 phase, as seen in Figures 6 and 7. Figure 5 reveals the imperfect crystalline structure of PET fibrils, compared to that of PA-6 and PA-66. This is probably due to the higher crystallizability of the polyamides. A similar supermolecular organization was observed by us earlier.[7–11]

Due to the miscibility of the two polyamides,[19] separate PA-6 or PA-66 microfibrils are not observed in the PA-66/PA-6 and PET/PA-6/PA-66 blends. Figure 7 shows a fibrillarlike structure on the PA-66/PA-6 bristle surface.

After thermal treatment at 245°C (i.e., above the T_m of PA-6), the morphology of the specimens remains almost the same—axially oriented PET or PA-66 fibrils (however, with improved crystalline structure) are distributed in a partially isotropized PA-6 and/or copolymer matrix, and in this way, a composite structure is maintained (Figs. 5–7). The preservation of the partial orientation of PA-6 could be related to the "preferred" crystallization of this polymer around and along the fibrillized PET and PA-66 during cooling after annealing. Such an epitaxial crystallization from the melt of PA-6 on the surface of poly(*p*-phenylene terephthalamide) filaments was observed by Kumamaru et al.[27] This type of crystallization is favored by the presence of chemical bonds between the components, restricting their separation, as well as by the nucleating effect of the fibrils,[23,27] which remain solid at 245°C. The columnlike structures formed during cooling follow to some extent the fibrillar orientation and contribute to the better compatibility of the components in the blends. It should be noted that this effect is best expressed at the PA-66/PA-6 interface in samples B-1 and C-1. In the latter case, the occurrence of cocrystallization is also possible (Figs. 5–7).

It could be assumed that the partially isotropized fractions would undergo some orientation in the axial direction under the action of an external mechanical field. However, the presence of chemical bonding between fibril and matrix would restrict the deformation ability of the matrix and, on the other hand, it would lead to some disorientation of the fibrillar phase. Flat-film patterns obtained from bristles which have been additionally drawn at $\sim$ 100% at room temperature (samples A-1, B-1, and C-1, Fig. 8) show little or no increase of orientation of the PA6-containing phase, compared to the drawn and annealed case (Fig. 5). This provides further evidence toward the existence of chemical bonds and cocrystallites in the blends.

As expected, the mechanical properties depend on the morphological changes in the blends. The orientation of the homopolymers after drawing leads to a strong increase of E and σ_t as compared to the as-extruded samples (Table III). The subsequent partial isotropization of the lower-melting fraction during thermal treatment at 245°C leads to a decrease of E by about 20% and of σ_t by about 50% while ε_u rises by almost 100% compared to the as-drawn blends (Table III). Nevertheless, the elastic modulus and tensile strength of these samples are much higher (3–5 times for E and 3–3.5 times for σ_t) than their respective values for PA-6 ($E \approx 1$ GPa, $\sigma_t \approx 45$ MPa) and for the as-extruded blends (Table III). The differences in the E values of samples A-1, B-1, and C-1 result from the chemical nature and the physical properties of the components, as well as from the amount of fibrillized material. The less stiff PA-66 fibrils reinforcing the PA-66/PA-6 composite impart a higher compliance, and, hence, a lower E, while the stiffer PET fibrils contribute to the higher E values of the PET/PA-6 composite (Table III). The presence of a relatively small amount (17% by volume) of fibrillized PET in the ternary blend leads to an increase by about 35% of the elastic modulus as compared to PA-66/PA-6 (Table III).

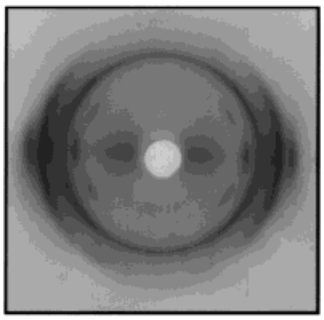

A

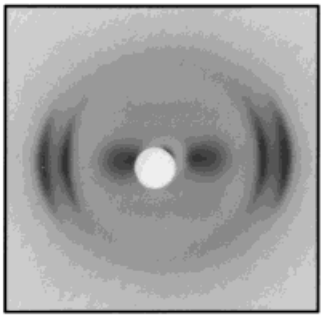

B

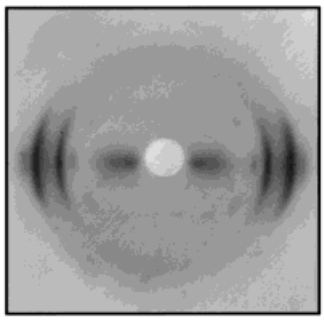

C

Figure 8 WAXS transmission patterns of PET/PA-6 (Sample A-1-1), PA-66/PA-6 (Sample B-1-1), and PET/PA-6/PA-66 (Sample C-1-1) blends, additionally drawn to $\varepsilon = 100\%$ after annealing at 245°C.

It should be noted that the weight, volume, and molar ratios of the components in the blends (and particularly in the thermally treated blends) do not correspond to their initial values, due to the chemical conversions discussed above. This decrease in the amount of the reinforcing elements as well as the changed chemical structure (copolymer) of the matrix influences the mechanical properties of the blends.

Concluding, we have shown that for various combinations of linear condensation polymers, using the techniques of *in situ* preparation of polymer/polymer composites, a wide variety of materials with tailored and desired properties can be obtained. Also, these materials were prepared from relatively inexpensive, commercial polymers.

M. Evstatiev and S. Petrovich gratefully acknowledge the hospitality of the Department of Chemical Engineering, University of Delaware, where most of the research was carried out. The visit was made possible through the support of the National Science Foundation (Grant # INT-9307812) and of the Bulgarian Ministry of Education and Science (Grant # X-542). Special thanks are also due to the Deutsche Forschungsgesellschaft (DFG-project FR 675/21-1) for supporting this research on microfibrillar composites.

REFERENCES

1. P. D. Frayer, *Polym. Compos.,* **8,** 379 (1987).
2. G. Kiss, *Polym. Eng. Sci.,* **27,** 410 (1987).
3. K. G. Blizard and D. G. Baird, *Polym. Eng. Sci.,* **28,** 17 (1988).
4. W. Brostow, *Polymer,* **31,** 979 (1990).
5. G. Crevecoeur and G. Groeninckx, *Polym. Compos.,* **13,** 244 (1992).
6. T. Sun, D. G. Baird, H. H. Huarg, D. S. Done, and G. L. Wilkes, *J. Compos. Mater.,* **25,** 788 (1991).
7. M. Evstatiev and S. Fakirov, *Polymer,* **33,** 877 (1992).
8. S. Fakirov, M. Evstatiev, and J. M. Schultz, *Polymer,* **34,** 4669 (1993).
9. S. Fakirov, M. Evstatiev, and S. Petrovich, *Macromolecules,* **26,** 5219 (1993).
10. S. Fakirov and M. Evstatiev, *Adv. Mater.,* **6,** 395 (1994).
11. M. Evstatiev, S. Fakirov, and K. Friedrich, *Appl. Comp. Mater.,* **2,** 93 (1995).
12. M. Kimura and R. S. Porter, *J. Polym. Sci. Polym. Phys. Ed.,* **21,** 267 (1983).
13. L. A. Utracki, *Polymer Alloys and Blends,* Hanser, Munich, Vienna, New York, 1989.
14. M. R. Kamal, M. A. Sahto, and L. A. Utracki, *Polym. Eng. Sci.,* **22,** 1127 (1982).
15. L. Z. Pillon and L. A. Utracki, *Polym. Eng. Sci.,* **24,** 1300 (1984).
16. S. Fakirov, in *Solid State Behavior of Linear Polyesters*

and Polyamides, J. M. Schultz and S. Fakirov, Eds., Prentice-Hall, Englewood Cliffs, NJ, 1990.
17. B. Wunderlich, *Polym. Eng. Sci.,* **18,** 431 (1978).
18. S. Gogolewski and A. Pennings, *Polymer,* **18,** 654 (1977).
19. T. S. Ellis, *Polymer,* **33,** 1469 (1992).
20. L. A. Utracki, M. R. Kamal, V. Tan, A. Catani, and G. L. Bata, *J. Appl. Polym. Sci.,* **27,** 1913 (1982).
21. J. M. Schultz, in *Proceedings of the 11th Annual Meeting, Polymer Processing Society,* Seoul, South Korea, March 27–30, 1995.
22. S. Balijepalli and J. M. Schultz, *Macromolecules,* **29,** 6601 (1996).
23. K. P. Gallagher, X. Zhang, J. P. Runt, G. Huynh-ba, and J. S. Lin, *Macromolecules,* **26,** 588 (1993).
24. J. Runt, L. Du, L. M. Martynowicz, D. M. Brezny, M. Mayo, and M. E. Hancock, *Macromolecules,* **22,** 3908 (1989).
25. A. A. Apostolov, S. Fakirov, B. Sezen, I. Bahar, and A. Kloczkowski, *Polymer,* **35,** 5247 (1994).
26. D. W. Ihm, A. Hiltner, and E. Baer, in *High Performance Polymers,* E. Baer and A. Moet, Eds., Hanser, Munich, 1991, p. 280.
27. F. Kumamaru, T. Oono, T. Kajiyama, K. Suehiro, and M. Takayanagi, *Polym. Compos.,* **4,** 135 (1983).